Studia Universitatis "Vasile Goldiş", Seria Ştiinţele Vieţii
Vol. 22, issue 1, 2012, pp. 83-93

PHASE SOLUBILITY STUDIES AND SCANNING ELECTRON MICROSCOPY OF DEXAMETHASONE INCLUSION COMPLEXES WITH B-CYCLODEXTRIN AND HYDROXYPROPYL B-CYCLODEXTRIN

Mariuca-Roxana GAVRILOAIA[*], Emma-Adriana BUDURA[1], Corina ARAMĂ[2], Mihai NITULESCU[1], Dumitru LUPULEASA[1]
[1] Pharmaceutical Technology Department, [2] Analytical Chemistry Department
„Carol Davila" University of Medicine and Pharmacy, Bucharest,

ABSTRACT
Dexamethasone, Dxm, is frequently used as an immunosuppressive to treat a broad range of autoimmune and inflammatory disorders, most of them occur locally and near the body surface. So, topical application could offer the advantage of delivering a drug directly to the affected surface, but barrier properties of skin limit the dexamethasone's permeability. Transdermal penetration could be improved by drug complexation with cyclodextrins.
The purpose of this paper is to analyze the formation of inclusion complexes of the drug with β-cyclodextrin and hydroxypropyl-β-cyclodextrin. Investigations were made by phase solubility diagrams and scanning electron microscopy in order to evaluate: the formation of 1:1 molar ratios, complexation efficiency, improved solubility, morphology and homogeneity samples. Huguchi and Connors method and fractal analysis were applied to compare the performances of the two final binary solutions.
KEYWORDS: dexamethasone, cyclodextrins, inclusion complex, phase solubility diagram, fractal analysis

INTRODUCTION

Dexamethasone, Dxm, is the most potent synthetic glucocorticoid which, unlike the naturally-occurring cortisol and corticosterone, has virtually pure glucocorticoid activity. It is frequently used as immunosuppressive to treat a broad range of autoimmune and inflammatory disorders and prevent graft rejection following bone marrow or organ transplantation [Aleem et al., 2008, Bibby et all, 2000]. Most inflammatory diseases occur locally and near the surface of the body, so topical application of Dxm on the inflamed site can offer the advantage of delivering a drug directly to the disease site to produce its local effect.

Dxm appears as a white powder, practically insoluble in water, but it is soluble in ethanol, methanol, acetone, dioxane and slightly soluble in chloroform [Brewster et al., 2007, Armatas et al., 2002, **Cázares** et al., 2010]. Its chemical structure is shown on Fig. 1. Dxm has a biological half-life in plasma of about 2-5 hours. However, the barrier properties of intact skin limit the Dxm permeability. The literature survey reveals that the solubility of Dxm can be enhanced by using cyclodextrins, Cds [Fansoon et al., 2010, Ozkan et al., 2000]. These cyclic oligosaccharides produced by enzymatic degradation of the starch have the ability to form inclusion complexes with a wide variety of guest molecules [Stella et al., 1997, Davies ER, 2008]. The complex formation is due to forces such as Van der Waals, hydrogen binding or hydrophobic interaction, but no covalent bonds exist between the Cd and its guest. All physicochemical properties of guest (solubility, thermal stability, melting point, chemical reactivity, spectroscopic and electrochemical) are changed. In the same time, Cd modifies transdermal drug penetration by complexation and drug release acceleration by enhancing the proportion of diffusible substance.

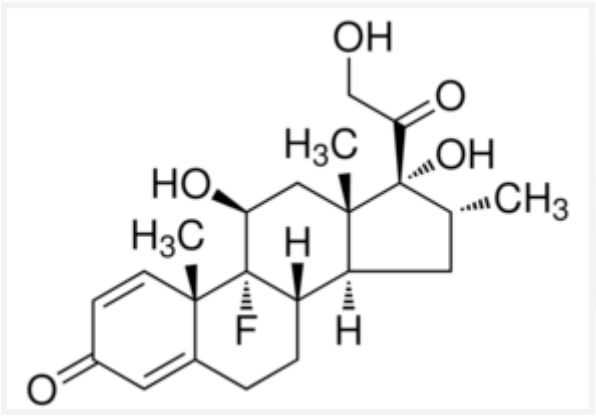

Fig. 1 Dexamethasone chemical structure

In the present study, we investigated the formation of two inclusion complexes: dexamethasone and β-cyclodextrin, Dxm – BCd, and dexamethasone with hydroxypropyl-β-cyclodextrin, Dxm – HPBCd,. The solubilization ability of Cd can be quantitatively evaluated by the phase solubility method developed by Higuchi and Connors [Vianna et al., 1998, Davies ER, 2008]. Some parameters such as: the value of molar ratio, stability constant, solubility, complexation efficiency could be evaluated from the solubility - phase diagram.

Besides physical and chemical parameters that are specific, the inclusion complex has an own physical

Correspondence: *Mariuca-Roxana GAVRILOAIA[*], „Carol Davila" University of Medicine and Pharmacy, Bucharest, Faculty of Pharmacy, 6 Traian Vuia St., 020956, Bucharest, Romania; e-mail: roxana21g@yahoo.com.*

structure. The new structure was investigated by using fractal geometry applied to the images from a scanning electron microscope, SEM. Fractal geometry was used because it was not possible for Euclidian geometry to describe the patterns of the objects from nature, the two inclusions complexes in our case. The fragments, existing on the complex images, were characterized by fractal dimension and lacunarity.

MATERIALS AND METHODS

Materials and sample preparations

Dexamethasone, β-cyclodextrin, and 2-hydroxypropyl-β-cyclodextrin were obtained from Fluka (Sigma - Aldrich Chemie GmbH, Germany), and all of them had a percentage purity greater than 97%. Ethanol used for the initial dilution of dexamethasone was of analytical grade. We used deionized ultrapure water for chromatography as a solvent (prepared using a Barnstead EasyPure RoDi apparatus). The substances were weighed with the Mettler Toledo precision balance - AT261, with a sensitivity of 0.01 mg.

The two Cds complexes were prepared by freeze drying at the same molar ratio, 1:1. In the first step, the inclusion complex BCd-Dxm was realized. 144,58 mg of BCd (127.39 mmols) were dissolved in 100 ml of distilled water. 15 ml of 96% ethanolic solution containing 50 mg (127.39 mmols) of Dxm was added stepwise to the aqueous solution of BCd. The suspension was stirred at 750 rpm, at room temperature, using the magnetic stirrer Heidolph MR 3001K, for about 7 h. After that, the final suspension was lyophilized for 12 h at -60°C, using the Christ ALPHA 1 – 2, B Braun Biotech International, Germany liophilizer (under vacuum, ice sublimates directly into water vapor).

The other inclusion complex, Dxm – HPBCd, was prepared in the same way, except the initial quantity of Cd. In this case, 177.07 mg of HPBCd were necessary to assure the same molar ratio, 1:1 with Dxm.

Methods

Phase solubility diagram

In this experiment, the Higuchi and Connors method was used to estimate the molar ratios, the apparent stability constants, and the complexation efficiencies of the two inclusion complexes. The method consists in evaluating the attenuation introduced by solutions with different concentrations of Cds in which Dxm was added in excess. Thus, 0.176 mmols (0.2 g) of BCd were dissolved in 15 ml of distilled water and 5 tubes were filled with the following amounts: 1 ml, 2 ml, 3 ml, 4 ml and 5 ml. Then, 0.2 mmols to 1 mmol of Dxm were added stepwise to five aqueous solutions of BCds, and distilled water was placed in each tube up to 5 ml. Also, 0.176 mmols (0.243 g) of HPBCd were prepared in the same way.

The two sorts of formulations, a total of 10 samples, were shaken for 24 h at 750 rpm, and room temperature 25 ± 2°C, using the Heidolph Vibramax 100 shaker. The substances were kept at rest about 6 hours, to reach equilibrium, and then filtered through a 0.45 μm nylon filter membrane (Whatman® PuradiscTM). The experiments were conducted in duplicate.

The concentration of the Dxm dissolved against water blank was measured spectrophotometrically by using the Perkin – Elmer LAMBDA 2 UV-VIS spectrometer in two steps. In the first step, the average molar absorbance of Dxm was measured for the following molar concentration of Dxm: .306 mM, .489 mM, and .611 mM. It is important to notice that the distances between wavelengths for maximum absorbance of Dxm, BCd, and HPBCd have be large enough, so the absorbance measurements will be independent. In the second step, the absorbance of the solutions from the ten tubes will be measured, and phase – solubility diagrams will be obtained. A linear dependence between Dxm concentrations and Cd concentrations, A_L curve, shows a 1:1 molar ratio. The following parameters could be evaluated from the concentrations curves or phase solubility diagrams [Higichi et al., 1965, Faula et al.,2007]:

- slope, m;
- the intrinsec solubility of Dxm, S_0;
- solubility constant, $K_{1:1}$:

$$K_{1:1} = \frac{m}{S_0(1-m)} \qquad (1)$$

- complexation efficiency, CE:

$$CE = K_{1:1}S_0 = \frac{m}{1-m} \qquad (2)$$

Fractal analyze of SEM images

The previous paragraph was based on indirect measurements. However, it is possible to investigate the pattern of separate and mixed substances, and to compare whether or not the mixed solution keeps the initial patterns. In many theoretical studies, biopharmaceutics and pharmacokinetics have been developed based on conceptions of homogeneity and linearity. The surface of drug particle, for example, is assumed to be smooth and its shape an ideal sphere. The real world is different, the irregularity and self-similarity under scale changes are the main attributes of the morphologic complexity of each object from microscope images. The shape of a self-similar object does not change when scales of measure change because any part of it might be similar to the original object. Size and geometric parameters of an irregular object are different when they inspected at increasing resolutions, which reveals more details. Fractal

geometry enables one to measure the fractal dimension, contour length, surface area, and other dimensional parameters of almost all irregular and complex objects.

The degree of irregularity is quantified by fractal dimension, *DF*. The most common method for the calculation of *DF* is called box counting [Dong P, 2009, Gavriloaia et al., 2011, Hagiwara et al., 1998,Karperein A, 2004]. It involves covering the object with circles or spheres of various radii. The minimum number of circles or spheres, $N(c)$ of size c needed to cover the object is calculated, and finally:

$$D = \lim_{c \to 0} \frac{\log N(c)}{\log (1/c)} \qquad (3)$$

Lacunarity or gap dimension, L_k, characterizes the way the 'gaps' are distributed in an image [Lee et al., 2000, Luo et al., 2009]. The gap dimension is, roughly speaking, a measure of the number of light or dark regions in an image. It is defined for a degree k by:

$$L_k = \left\langle \left| \frac{f_{m,n}}{\langle f_{m,n} \rangle} - 1 \right|^k \right\rangle^{1/k}, \qquad (4)$$

where

$$\langle f_{m,n} \rangle = \frac{1}{N} \sum f_{m,n}$$

denotes the mean value. In this paper, an average of local lacunarities of the degree $k = 2$ is measured by using the gliding box algorithm based on the analysis of mass distribution, *M*, in the set [Hagiwara et al., 1998]. The gliding box is moved one space unit at a time. The box mass *m* is recounted till the whole region is traversed thus producing a frequency distribution of box masses over a number *n* of boxes. This distribution is converted into a probability distribution $f_{m,n}$, by dividing *M* by the total number of boxes, *n* [Lee et al., 2000].

The morphology of samples was determined using the scanning electron microscope, **FEI Nova NanoSEM 630**. Nova NanoSEM 630 series is a family of ultra-high resolution field-emission SEMs which is specifically configured to get the most information out of the largest selection of samples, down to the nanometer level. Although this electronic device can provide up to 1 nm resolution, the samples investigated by us had a maximum 500 nm resolution. The images were registered at magnifications between 600x - 80.000x. On the same support, small amounts of each substance were placed on an adhesive substrate, and then covered with a thin layer of gold. Eight images with different resolutions were taken for each substance.

RESULTS AND DISCUSSION

Phase solubility diagram

The first set of measurements were performed to determine the Dxm mean absorbance, and wavelength to which absorbance has maximum value. The results founded for the three solutions of Dxm having the following molar concentrations: 0.306 mM, 0.489 mM and 0.611 mM, are presented in Tab. 1. The average value of molar absoptivity, ε, is about 1.83 mM^{-1}. The dependence of absorption versus wavelength is shown in fig. 2, for the central value of Dxm solution concentration. The maximum of absorption occurs at 241.5 nm (UV spectrum), which is far enough from the corresponding values of maximum absorptions of BCd or HPBCd, less than 200 nm [Luo et al., 2009, Okzan et al., 2000].

The solubilization ability of Cds can be quantitatively evaluated by the phase solubility method developed by Higuchi and Connors [5]. The phase solubility diagrams at 25 °C were obtained by plotting the apparent equilibrium concentrations of Dxm against BCd and HPBCd concentrations.

Tab. 1 Molar absorptivity of dexamethasone

Dexamethasone			
Molar concentration [mM]	Absorbance	Molar absorptivity, ε [mM^{-1}]	Lungimea de unda [nm]
0.305732	0.522	1.707375	241.4
0.489172	0.875	1.78873698	241.5
0.611465	1.219	1.99357292	241.6
Average values		**1.82989497**	**241.5**

CThe maximum values of absorbances for five molar concentrations of BCd solutions saturated with Dxm are presented in Tab. 2. In fig. 3 is presented the variation of BCd solution absorbance for central value of concentration. By using the value of the molar absoptivity from previous step, the molar concentration of Dxm for each solution is evaluated, and presented in the same table. The results were plotted in Fig. 4.

The apparent solubility of Dxm increased as function of βCD concentration up to 1.2 mM, corresponding to the aqueous solubility of BCd. A linear interpolation could be done, $r^2 = 0.9978$, and from the regression equation, the slope and intrinsic solubility were determined (the criterion of admissibility is $r^2 \geq 0.995$, so the method was found linear in the range of 2.0 to 12.0 mM).

The linear relation between Dxm solubility and BCd and the slope value, lower than one (0.0951), indicate an A_L-type phase-diagram, defined by Higuchi and Connors.

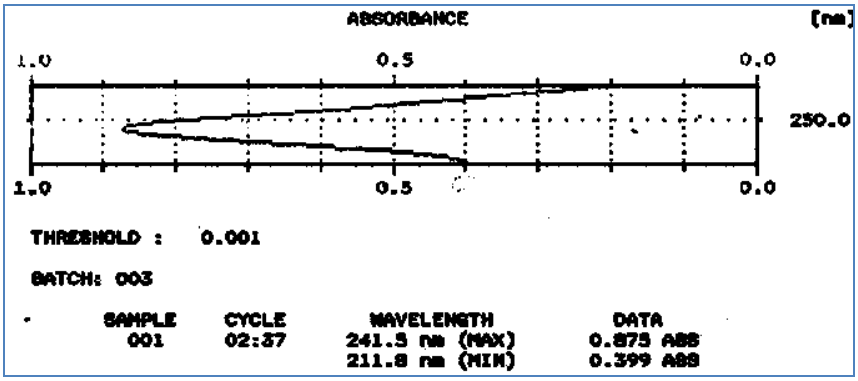

Fig. 2 Dexamethasone absorbace versus wavelength, 0.96 mg/ml

This diagram is characteristic of 1:1 complexation between the guest (Dxm) and host (BCd) molecules and suggests that water soluble complex was formed in solution [5, 18]. Furthermore, Dxm solubility increased about 19.2 fold when BCd was used in concentration of 11.72 mM.

Tab. 2 The phase solubility diagram parameters of the inclusion complex formed between Dxm and BCd

Molar concentration a BCd, [mM]	Absorbance, A	Molar concentration of Dxm M=A/ε, [mM]	Slope, m	Intrinsec solubility, S_0 [mM]	Stability constant, $K_{1:1}$ [M^{-1}]	Complexation efficiency, CE
2.34	0.393	0.2148	0.0951	0.06	1751.6	0.1051
4.63	0.855	0.4672				
7.02	1.231	0.6727				
9.46	1.543	0.8432				
11.72	2.104	1.1498				

The results for the inclusion complex Dxm - HPBCd are presented in Tab. 3, the variation of HPBCd solution absorbance for central value of concentration, 7.02 mM, is shown in fig. 4, and data are plotted in fig. 7. By linear interpolation, $r^2 = 0.9978$, the slope and intrinsic solubility were found. The slope of regression line is a little bit higher than the slope from the previous diagram, but smaller than 1, suggesting an A_L-type phase-diagram, according to Higuchi and Connors.

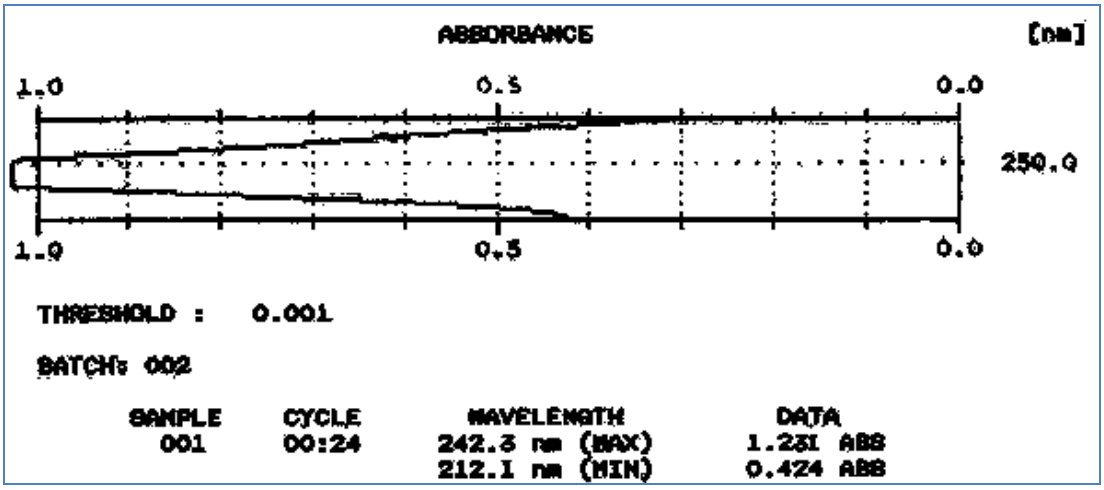

Fig. 3 The absorbance of 7.02 mM BCd - Dxm versus wavelength

Tab. 3 The phase solubility diagram parameters of the inclusion complex formed between Dxm and HPBCd

Molar concentration a HPBCd, [mM]	Absorbance, A	Molar concentration of Dxm M=A/ε, [mM]	Slope, m	Intrinsec solubility, S_0 [mM]	Stability constant, $K_{1:1}$ [M^{-1}]	Complexation efficiency, CE
2.34	0.545	0.2978	0.1617	0.07	2755.6	0.1929
4.63	1.378	0.7530				
7.02	2.25	1.2296				
9.46	3.04	1.6613				
11.72	3.2	1.7487				

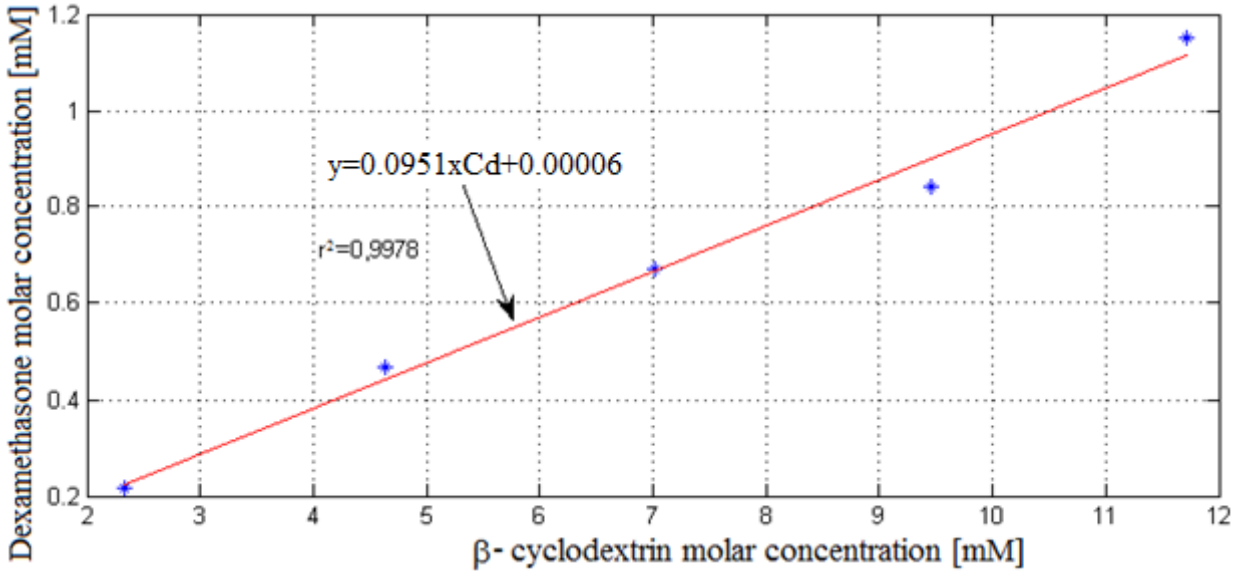

Fig. 4 The solubility phase diagrams for the inclusion complexes Dxm- BCd

The apparent stability constant, $K_{1:1}$, of Dxm-BCd complex (1:1) was calculated as 1751.6 M^{-1} from the linear plot of the phase solubility diagram.

The computed values, the stability constant, $K_{1:1}$ is 2755, and complexation efficiency is 0.1929. This inclusion complex improves Dxm solubility about 24.97 fold.

All parameters of the HPBCd – Dxm inclusion complex, computed from the phase diagram curve, are higher than BCd-Dxm complex parameters. The complexation efficiency shows that not all amount of substances formed the inclusion complex, but both complexes are very stable.

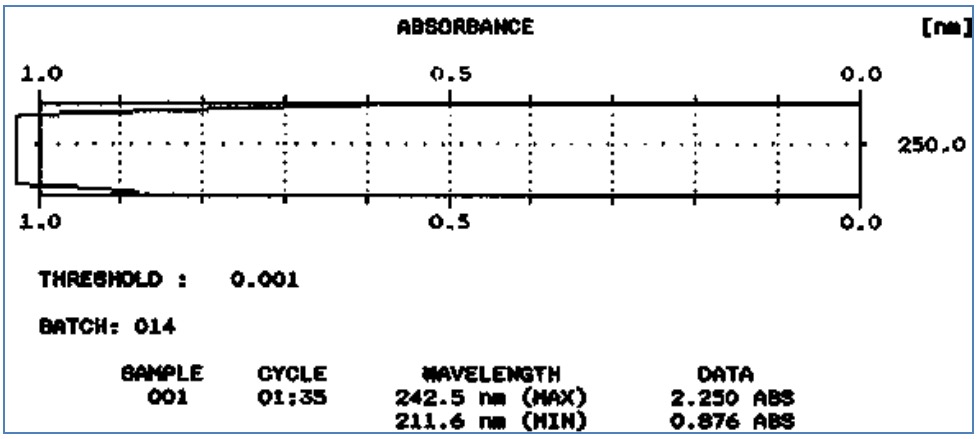

Fig. 5 The absorbance of 7.02 mM HPBCd and Dxm versus wavelength

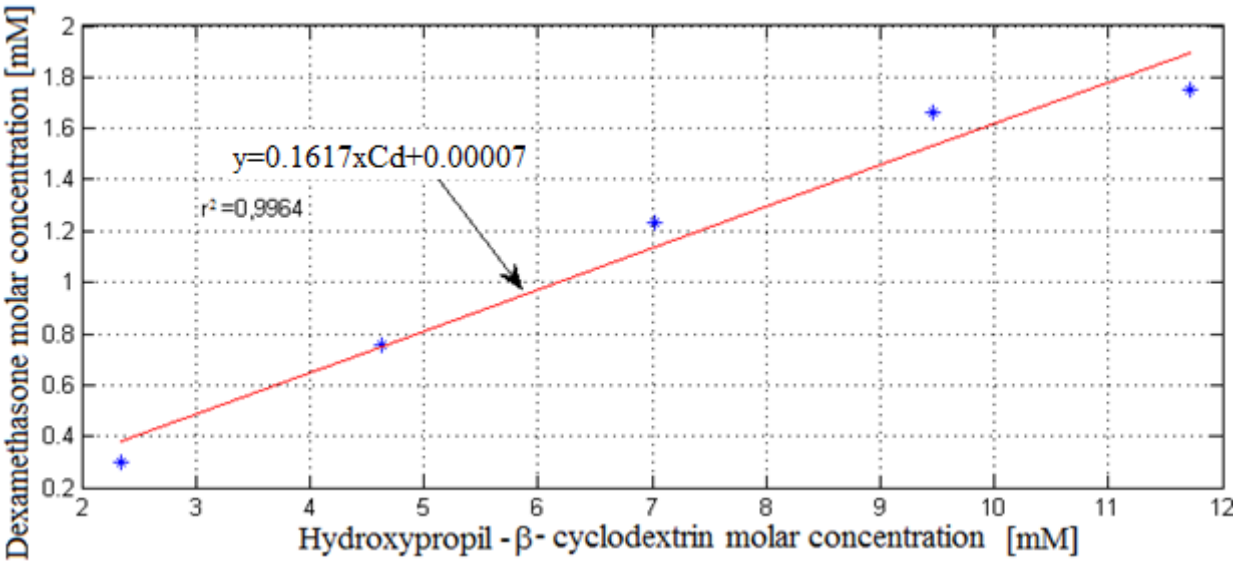

Fig. 6 The solubility phase diagrams for the inclusion complexes Dxm- HPBCd

Fractal analysis of SEM images

The morphologic complexity of the five substances was investigated by SEM. Eight images of 1024×885 pixels were taken from each materials with following resolutions and magnifications: 600x-100 μm/div, 1200x - 50 μm/div, 2400x-20 μm/div, 5000x – 10 μm/div, 10.000x - 5 μm/div, 20.000x - 3 μm/div, 40.000x - 1 μm/div, 80.000x - 500 nm/div., fig. 9-11.

Dxm is characterized by the presence of homogenous crystalline particles, having about parallelepiped shapes, with various sizes between 1 and 10 μm, Fig. 7. The whole picture shows a heterogeneous substance.

The HPBCd SEM images are shown in fig. 8. Many spherical particles, with an amorphous character can be seen, but the whole picture shows a heterogeneous substance.

The images from fig. 9 show how the BCd can be seen at SEM with different resolutions. The substance has an amorphous and heterogeneous character. Also, these features can be noticed on images in Fig. 10 corresponding to BCd - Dxm inclusion complex.

The images with different resolutions of HPBCd -Dxm inclusion complex are presented in Fig. 11. Some small and broken spherical particles could be seen, but all images have a heterogeneous content.

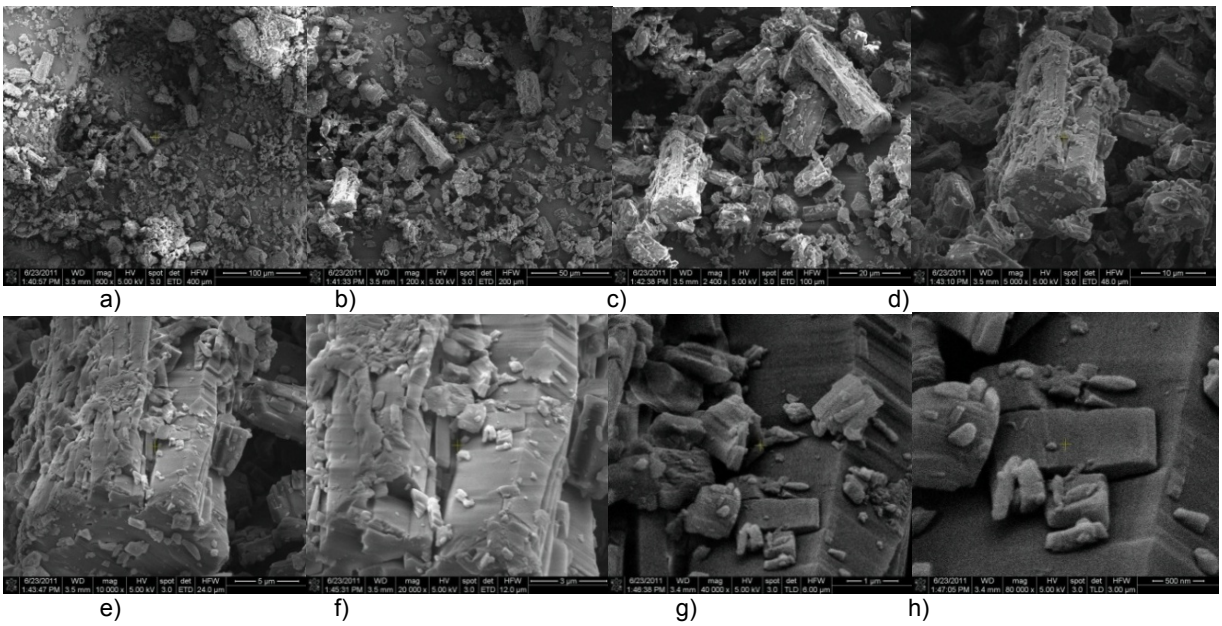

Fig. 7 Dexamethasone SEM images, magnifications: 600x (a), 1200x (b), 2400x (c), 5000x (d), 10.000x (e), 20.000x (f), 40.000x (g), 80.000x (h)

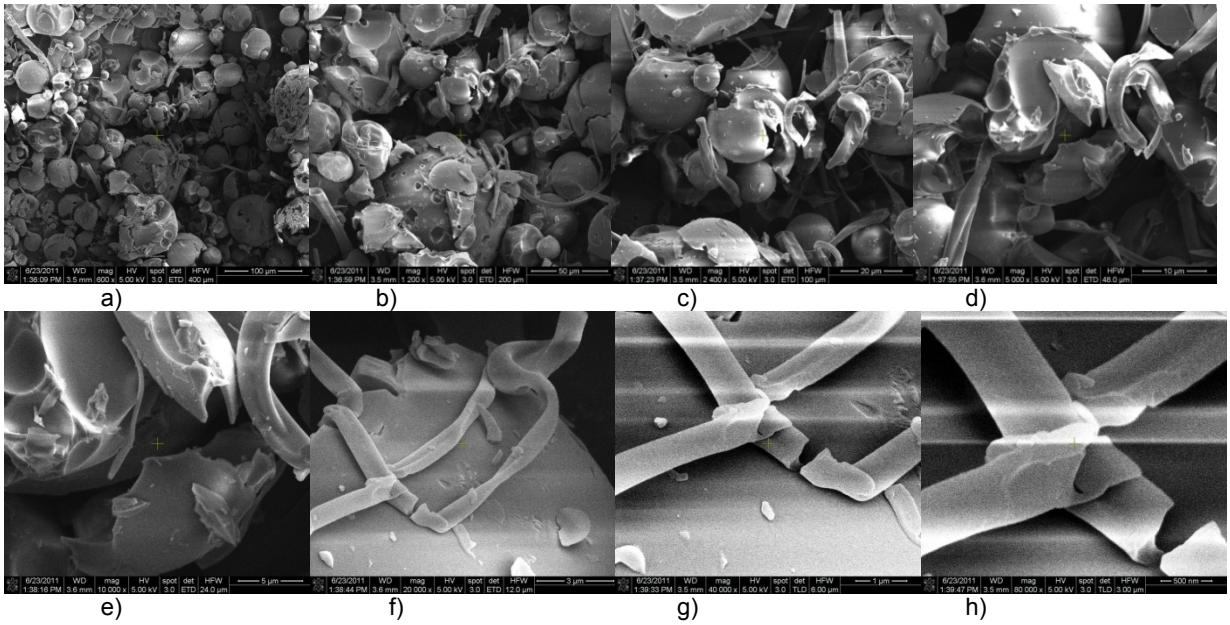

Fig. 8 HPBCd SEM images, magnifications: 600x (a), 1200x (b), 2400x (c), 5000x (d), 10.000x (e), 20.000x (f), 40.000x (g), 80.000x (h)

The images of the inclusion complexes, Fig 10-11, are completely different from those of component substances, Fig 7-9, showing that new substances formed. Meanwhile, one can see that there are small particles that are similar to the original form, thus the complexation has not been complete. These observations are only of qualitative nature. An investigation of quantitative analysis can be done using fractals. In fig. 12 (a)-(d) is given an example for fractal analysis of Dxm image having 20 μm/div resolution, fig. 11a. The microscopy images were analyzed with personal software. The contour of objects was obtained by choosing the median value for the threshold of grey image, Fig. 12b. The irregularity and self-similarity under scale changes are the main attributes of objects from microscope images. In other words, the shape of a self-similar object does not change when scales of measure change because any part of it might be similar to the original object. Size and geometric parameters of an irregular object, however, differ when inspected at increasing resolution, which reveals more details. Analyses of these irregular shapes and structures could be done by application of the fractal geometry principles, enables one to measure the fractal dimension, contour length, surface area, and other dimensional parameters.

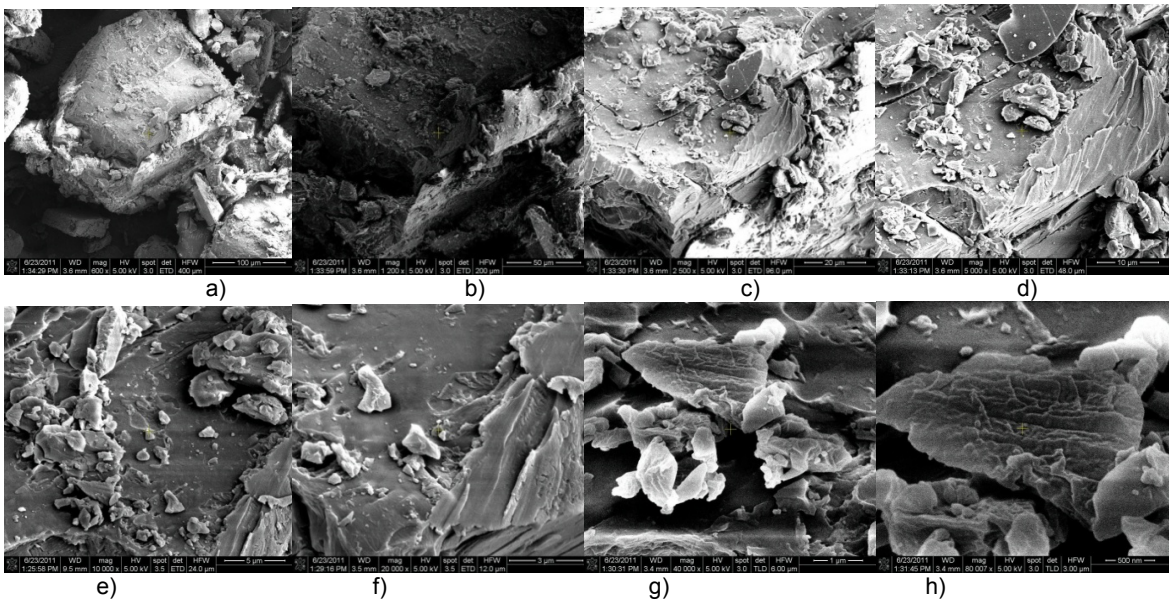

Fig. 9 BCd SEM images, magnifications: 600x (a), 1200x (b), 2400x (c), 5000x (d), 10.000x (e), 20.000x (f), 40.000x (g), 80.000x (h)

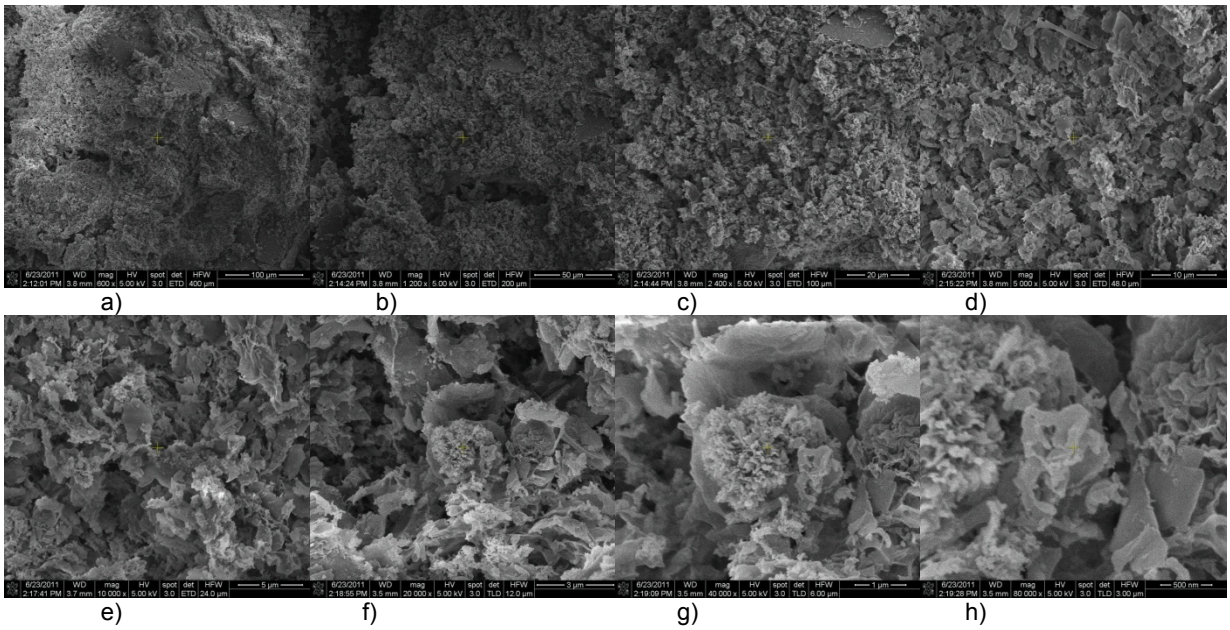

Fig. 10 SEM images of the inclusion complex BCd -Dxm, magnifications: 600x (a), 1200x (b), 2400x (c), 5000x (d), 10.000x (e), 20.000x (f), 40.000x (g), 80.000x (h)

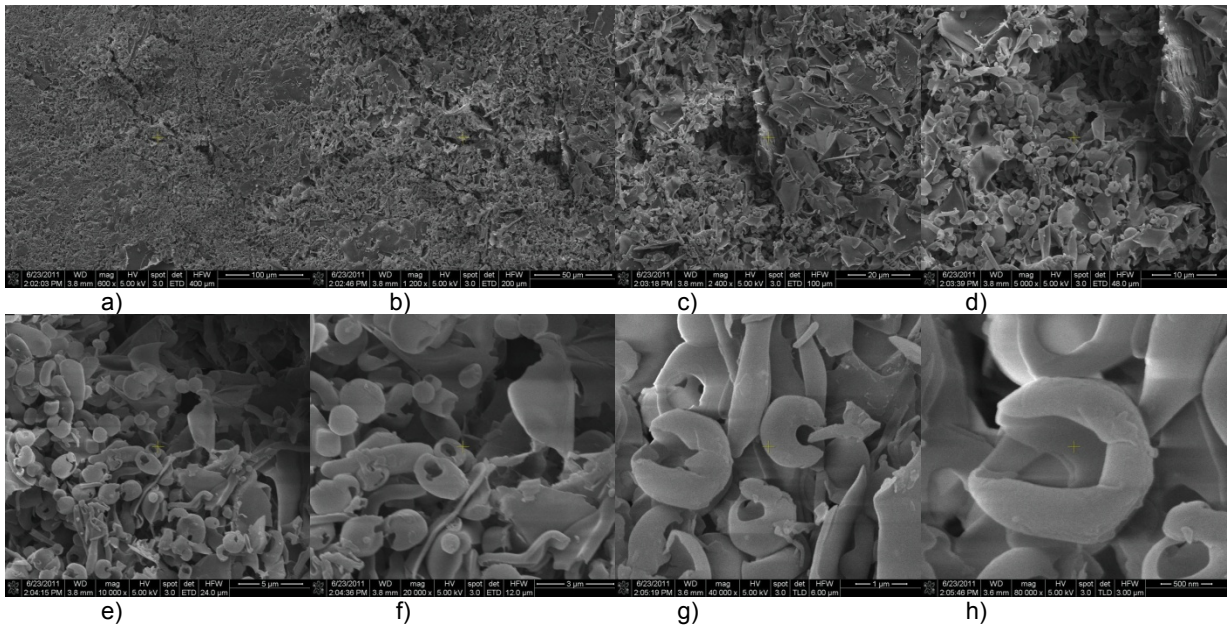

Fig. 11 SEM images of the inclusion complex HPBCd -Dxm, magnifications: 600x (a), 1200x (b), 2400x (c), 5000x (d), 10.000x (e), 20.000x (f), 40.000x (g), 80.000x (h)

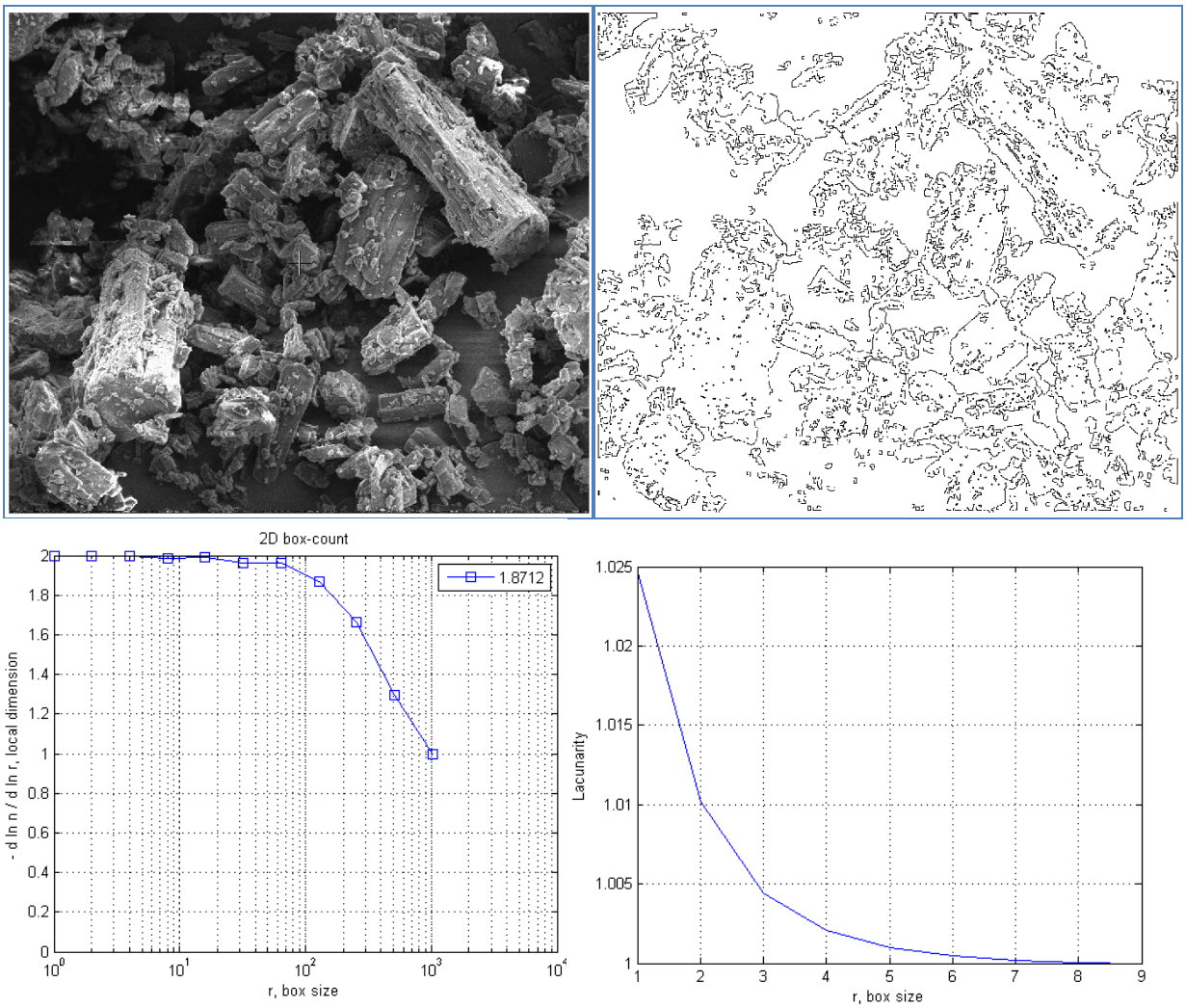

Fig. 12 Example of fractal analysis of Dxm sample, image has 20 μm/div resolution

DF value of the sample image was computed using the box counting method. The basics of the box counting method are the placement of several grids of decreasing size over an image and the number of boxes containing pixels is counted for each grid. The *DF* is based on the calculation of the scaling rule, given by (1), and it is the same with the slope of number of boxes dependence, the curve shown in Fig. 12 (c). The evolution of "gaps" in image, lacunarity, versus gliding box dimension is presented in Fig. 12(d). The values of DF and lacunarity for all images of samples are presented in Tab.4.

Tab. 4

	Dxm	HPBCd	BCd	BCd-Dxm	HPBCd-Dxm
DF	1.786±0.026	1.792±0.031	1.839±0.018	1.805±0.025	1.882±0.034
Lacunarity	1.02-1.43	2.04-2.37	1.58-1.86	1.31-1.39	1.73-2.08

Geometrical complexity of SEM images for five different substances was investigated by their FDs evaluation versus eight possible scale resolutions. FD is very important for any recognition or classification process. FDs are different, but there are resolutions were they have similar values, even if they have different appearances. Therefore, a new parameter, lacunarity as measure of spatial heterogeneity, was used to differentiate between images. From this point of view, the two inclusion complexes seem to be more homogeneous than separate components, but of them, Dxm HPBCd inclusion complex seems to be more heterogeneous.

CONCLUSIONS

Two cyclodextrin inclusion complexes with Dxm were studied. A natural cyclodextrin - BCd, and a synthetic one - HPBCd were used to prepare the inclusion complexes by lyophilization technique. In order to compare the formation of inclusion complexes, solubility, stability, and complexation efficiency, the phase solubility diagrams were computed, and Higuchi and Connors method was applied.

This study indicated that Dxm formed stable and water soluble inclusion complexes with the two cyclodextrins. The amount of Dxm dissolved in their aqueous solutions is a linear increase up to 12 mM molar concentrations, classified to be as A_L type, indicating the formation of 1:1 molar ratio inclusion complexes. The two CDs increase the aqueous solubility of Dxm. Their stability constants are very high and confirm the fact that the final complexes are relatively stable according to values from [6, 8]. The value of complextion efficiency indicates that not all amounts of substances were used to form the inclusion complex, a part of them were not included, and so, there were not complete complexations.

The evaluating the morphology of the two inclusion complexes, formation of inclusion complexes, and the existence of the initial substances in the final product were possible using SEM technique and qualitative and quantitative evaluations. By visual observations, the shape, size, and structure of the initial substances were modified, showing that the final products are not only simple mixtures, but new products. Fractal dimension and lacunarity from the fractal analyses gave us the possibility to do a quantitative evaluation of complexity of the geometrical shapes, heterogeneity and homogeneity of complex has now been formed. The differences between initial and final product structures show the formation of inclusion complexes, and also the existence of some non-complex products.

All our studies indicated that BCd and HPBCd enhance the solubility of Dxm, a drug substance practically insoluble in water, and the parameters of HPBCd - Dxm inclusion complex are better than of BCd-Dxm inclusion complex for topical applications.

ACKNOWLEDGEMENT

We thank Mr. Andrei Dinescu (**National Institute for Research and Development in Microtechnologies -IMT – Bucharest)** for the valuable help in SEM investigations.

REFERENCES

Aleem O., Kuchekar B., Pore Y., Late S., Effect of β-cyclodextrin and hydroxypropyl-β-cyclodextrin complexation on physicochemical properties and antimicrobial activity of cefdinir, J.Pharm.Biomed. Anal, 47, 535-540, 2008,

Armatas G.S., Kolonia K.M., and Pomonis P.J., Morphometry of porous solids: lacunarity, fractal dimensions, connectivity, and some topological similarities with neurons. Langmuir, 18, 26, 3552-3558, 2002,

Bibby D. C., Davies N . M., and Tucker I. G., Mechanisms by which cyclodextrins modify drug release from polymeric drug delivery systems. Int. J. Pharm. 197:1–11, 2000,

Brewster M.E., Loftsson T., Cyclodextrins as pharmaceutical solubilizers, Adv.Drug Deliv.Rev., 59, 645-666, 2007,

Higuchi T., Connors K.A., Phase-solubility techniques, Adv.Anal.Chem.Instr., 4, 117-122, 1965,

Cázares D. J., Fernández C.B., Pascual A. C., Rondero A., G., Guerrero D.Q., Castellano L., Merino V., Kalia V., Transdermal iontophoresis of dexamethasone sodium phosphate in vitro and in vivo: Effect of experimental parameters and skin type on drug stability and transport kinetics, European Journal of Pharmaceutics and Biopharmaceutics Volume 75, Issue 2, June, p 173-178, 2010,

Davies E.R., Handbook of Texture Analysis, Chapter 1—Introduction to texture analysis, Imperial College Press, London, UK, 2008,

Dong P., Lacunarity analysis of raster datasets and 1d, 2d, and 3d point patterns. Computers and Geosciences, 35, 2009,

Fansook P., Ritthidej G., Ueda H., Stefánsson E., Loftsson T., γCD/HPγCD Mixtures as Solubilizer: Solid-State Characterization and Sample Dexamethasone Eye Drop Suspension, J Pharm Pharmaceut Sci (www.cspsCanada.org) 13(3), p 336-350, 2010,

Faula D., Oliveira D., Tedesco A.C., Bentley M. V., Enhancing effect of modified beta-cyclodextrins on in vitro skin permeation of estradiol, Revista Brasileira de Ciências Farmacêuticas, Brazilian Journal of Pharmaceutical Sciences, vol. 43, n. 1, jan./mar., 2007,

Gavriloaia M.R, Creţu E.A, Lupuleasa D, Infrared studies on the thermal efect of topical glucocorticoids/ cyclodextrins complexes, ACTA MEDICA MARISIENSIS, Volume 56, Supplement 2, The XIVth National Congress of Pharmacy from Romania, Tîrgu-Mureş, October 13th – 16th, 2010, Official publication of the University of Medicine and Pharmacy of Târgu Mureş, ISSN 2068-3324, pag. 100, 2010.

Hagiwara T., Kumagai H., and Nakamura K., Fractal analysis of aggregates in heat-induced BSA gels. Food Hydrocolloids, 12, 1, p 1756-1763, 1998,

Karperien A., FracLac advanced user's manual, Charles Sturt University, Australia, 2004,

Lee T., Atkins,M. S., A new approach to measure border irregularity for melanocytic lesions, Medical Imaging 2000: Image Processing, Proceedings of SPIE Vol. 3979, p 250-256, 2000,

Luo L., and Lin H., Lacunarity and fractal analyses of soil macropores and preferential transport using micro-X-ray computed tomography. Vadose Zone Journal, 8, p 233-241, 2009,

Ozkan Y., Atay T., Dikmen N., Işimer A., Aboul-Enein H.Y., Improvement of water solubility and in vitro dissolution rate of gliclazide by complexation with β –cyclodextrin, Pharm. Acta Helv., 74, Apr;74(4):365-70. 2000,

Sonka M., Hlavac V., Boyle R., Texture, in: Image Processing, Analysis, and Machine Vision, third ed., Thomson Learning, Ontario, Canada, 2008,

Stella V. J., Rajewski R. A., Cyclodextrins: Their future in drug formulation and delivery, Pharm. Res., May; 14(5): 556-5671997:

Vianna R. F. L., Bentley M. V., Ribeiro L. B. G et al. Formation of cyclodextrin inclusion complexes with corticosteroids: their characterization and stability. Int. J. Pharm. V. 167, p.205-213, 1998.